PFC/JA-90-26

Dynamic Stability of Edge Cooled Superconducting Tapes

J. Schwartz, J. P. Freidberg, J. E. C. Williams

July 1990

MIT Plasma Fusion Center
Cambridge, MA 02139

Submitted for publication in: Cryogenics

Dynamic stability of edge cooled superconducting tapes

J. Schwartz,* J. P. Freidberg, J. E. C. Williams

MIT Plasma Fusion Center, 167 Albany Street, Cambridge, MA 02139 USA

*Permanent address: University of Illinois, Department of Nuclear Engineering, 214 Nuclear Engineering Laboratory, 103 S. Goodwin, Urbana, IL 61801, USA

Abstract

The flux jump stability characteristics of an edge cooled tape superconductor are analyzed. Two simple cases (no stabilizer, perfect stabilizer) are considered to establish the lower and upper bounds of the stable operating space. The generalized case is then solved in the interesting limit where the tape thickness is small compared to its width and compared to the one dimensional condition of Hart. The 2-D analysis indicates that finite thermal diffusion in the superconductor can play a significant role for $w_0/d < 100$, where w_0 is the half width of the tape and d is the thickness of the superconductor.

Introduction

The penetration of magnetic flux into a superconductor is a dissipative process. As flux penetrates a superconductor, heat is released, increasing the local superconductor temperature and reducing the critical current density, J_{max}. In a Type II superconductor, the ability to shield magnetic field is proportional to J_{max}. Thus, a decrease in J_{max} leads to further flux penetration, creating a positive feedback system. If the feedback is larger than the ability of the superconductor to disperse heat, the perturbation grows and catastrophic (unstable) flux jumping occurs.

When a component of magnetic field is normal to the wide face of a tape superconductor, self-stabilization is particularly difficult and dynamic stabilization is necessary. There are two options for the geometry of a dynamically stabilized tape conductor: face cooled and edge cooled (Fig. 1). Although face cooling can be quite stable, it has serious

drawbacks for large, high field, magnet systems. As coolant is required for each thickness of superconductor, a stack of conductors can be stabilized only if spacers are provided to allow coolant flow between each layer. Furthermore, if there is any component of magnetic field in the plane of the tape normal to the direction of current flow, then there is a Lorentz force normal to the face of the tape. This force must be transferred to a structure at the edges of the tape through shear, through spacers, or through a structural membrane that provides a load path from the face of the tape to external structure. A structural membrane usually provides the best mechanical support, although it reduces the wetted perimeter of the conductor and thus the stability. Even under the best conditions face cooling is not very desirable in high field magnets because of the structural requirements.

In contrast edge cooling offers substantial mechanical advantages. However, it is more susceptible to instability than face cooling. With high field magnets as the ultimate goal, it thus makes sense to analyze the stability of edge cooled magnets in realistic geometries to accurately predict the design boundaries for safe operation. That is the goal of the present work.

In reviewing the literature, we note that the theory of flux jump stability has received considerable attention in the past.[1-9] Simple one dimensional isothermal and adiabatic models have been investigated as well as sophisticated two dimensional composite models. An excellent review of the subject has been given by Wilson.[9] Our mathematical analysis is similar to the two dimensional studies of Kremlev et al.[8] The main difference is that in our studies the superconductor and stabilizer must be treated as separate regions. Specifically, Kremlev et al use a cross section averaged relation between E and J, which ultimately leads to a single region description of the "averaged" material. Since their interests are primarily in composites with nearly uniform current density over the filament cross sections, this is indeed a reasonable approximation. However, our interest is focussed on tape wound magnets where the thermal gradients across the superconductor play a major role. Thus, it is cricital to treat the conductor and stabilizer regions separately.

In the present work, the linearized stability of an edge cooled tape is investigated in a two dimensional, multi-region geometry by means of an expansion in the ratio of

tape thickness to width. Included in the analysis is a discussion of two limiting cases corresponding to (1) no stabilizer and (2) perfect stabilizer. This provides lower and upper stability bounds for the general two dimensional case. A simple nonlinear theory is also presented demonstrating the behavior in the vicinity of the somewhat singular linear stability boundary. The results reduce to previously derived boundaries in the appropriate limits. The most interesting new result is the discovery that finite thermal diffusion in the superconductor can play an important role when $w_0/d \lesssim 100$ where w_0 is the half width of the tape and d is the thickness of the superconductor. This effect leads to a more stringent stability boundary than previously predicted.

General equations

The general equations governing the flux jump instability are Maxwell's equation and the heat equation

$$\nabla \times \mathbf{E} = -\frac{\partial \mathbf{B}}{\partial t}$$

$$\nabla \times \mathbf{B} = \mu_0 \mathbf{J} \tag{1}$$

$$C\frac{\partial T}{\partial t} = \nabla \cdot (\kappa \nabla T) + \mathbf{E} \cdot \mathbf{J} \ .$$

Consider a two dimensional (x,y) geometry. Substituting the vector potential $\mathbf{A} = A(x,y,t)\mathbf{e}_z$ for the magnetic and electric fields

$$\mathbf{B} = \nabla A \times \mathbf{e}_z \tag{2}$$

$$\mathbf{E} = -\frac{\partial A}{\partial t}\mathbf{e}_z \tag{3}$$

one obtains

$$C\frac{\partial T}{\partial t} = \kappa \nabla^2 T - J\frac{\partial A}{\partial t} \tag{4}$$

$$\nabla^2 A = -\mu_0 J \ . \tag{5}$$

For the superconductor $J = J(T, |\nabla A|)$ while for the stabilizer $J = -(1/\hat{\eta})\partial A/\partial t$ where $\hat{\eta}$ is the resistivity. In the analysis, the dependence of J on $|\nabla A|$ is neglected relative

to the dependence upon T when solving Eqs. (4) and (5) in the superconductor; that is $J(T, |\nabla A|) \approx J(T)$. For a superconductor operating at an equilibrium temperature T_0, J is modeled as

$$J(T) = \begin{cases} J_c(1 - T/T_c) & T > T_0 \\ J_c(1 - T_0/T_c) & T < T_0 \end{cases} \tag{6}$$

as shown in Fig. 2. If the temperature increases (e.g. due to flux penetration) then J decreases. If T decreases during operation, however, J does not increase and flux is not expelled from the superconductor. This asymmetric response is crucial in determining the stability boundaries.

Following Bean's critical state model[2] it is assumed that in steady state (1) $J = 0$ in the stabilizer and (2) $J = J(T_0)$ or $J = 0$ in the superconductor; only two values of J are allowed in the superconductor. See Fig. 3a. Note that the division between the two regions requires a complicated "free boundary" analysis. In principle this surface is determined by simultaneously requiring A and $\mathbf{n} \cdot \nabla A$ to vanish on the boundary. To simplify the analysis, a quasi-one-dimensional approximation is made but *only* for the steady state solution. The dynamics are treated two dimensionally. The approximate steady state model is illustrated in Fig. 3b. The main difference between the solutions is the appearance of small steady state surface currents along the stabilizer-superconductor interface. These make minor modifications to the steady state solution and have a negligible impact on the dynamics.

Hereafter, the stabilized superconductor analysis is treated as the three region problem corresponding to Fig. 3b. In Region 1 supercurrent flows such that Region 2 is completely shielded. Region 3 is the stabilizer which has field but no steady state current.

Boundary conditions

In Fig. 3b, $x = w_0$, $y = 0$ and $y = d + \hat{d}$ are symmetry planes and the unit cell conductor shown is one-fourth of the actual conductor. The first conditions are related to symmetry and are given by

$$\begin{aligned}
&\frac{\partial T_1}{\partial y}(x,0) = \frac{\partial T_2}{\partial y}(x,0) = \frac{\partial T_3}{\partial y}(x, d+\hat{d}) = 0 \\
&\frac{\partial T_2}{\partial x}(w_0,y) = \frac{\partial T_3}{\partial x}(w_0,y) = 0 \\
&\frac{\partial A_1}{\partial y}(x,0) = \frac{\partial A_3}{\partial y}(x, d+\hat{d}) = 0 \\
&\frac{\partial A_3}{\partial x}(w_0,y) = 0 \ .
\end{aligned} \tag{7}$$

Next, consider the superconductor/stabilizer interface ($y = d$). Across this boundary jump conditions must be satisfied which can be expressed as

$$\begin{aligned}
[\![T]\!]_{y=d} &= [\![\kappa \frac{\partial T}{\partial y}]\!]_{y=d} = 0 \\
[\![A]\!]_{y=d} &= [\![\frac{\partial A}{\partial y}]\!]_{y=d} = 0 \ .
\end{aligned} \tag{8}$$

The next boundary is $x = 0$. Here, the exact thermal boundary condition is

$$\kappa \frac{\partial T}{\partial x}(0,y) = h\,[T(0,y) - T_B] \tag{9}$$

where h is the heat transfer coefficient from the conductor to the coolant and T_B is the bulk temperature of the coolant. Under normal conditions,

$$\kappa / hw \ll 1 \tag{10}$$

and

$$hw/\hat{\kappa} \ll 1 \tag{11}$$

where $\partial T/\partial x \sim T/w$, w is the penetration depth of the field into the superconductor (Fig. 3) and κ and $\hat{\kappa}$ are the thermal conductivities of the superconductor and stabilizer. Thus, to a good approximation the thermal boundary conditions become

$$T_1(0,y) \approx T_B$$

$$\frac{\partial T_3}{\partial x}(0,y) \approx 0 \ . \tag{12}$$

The magnetic boundary conditions at $x = 0$ depend upon the spacing between conductors within the coil (see Fig. 4). Requiring the total flux to be conserved during a perturbation, leads to the boundary condition

$$\begin{aligned} \frac{\partial A_1}{\partial x}(0,y) - \frac{2A_1(0,y)}{\ell} &= -B_0\left(1+\frac{w}{\ell}\right) \\ \frac{\partial A_3}{\partial x}(0,y) - \frac{2A_3(0,y)}{\ell} &= -B_0\left(1+\frac{w}{\ell}\right) \end{aligned} \tag{13}$$

where ℓ is the spacing between the conductors and B_0 is the external magnetic field. Since $\partial A/\partial x \sim A/w$ the boundary condition may be simplified according to the size of w/ℓ. In the limit

$$\frac{w}{\ell} \ll 1 \tag{14}$$

the boundary condition becomes

$$\frac{\partial A_1}{\partial x}(0,y) \approx \frac{\partial A_3}{\partial x}(0,y) \approx -B_0 \ . \tag{15}$$

The final conditions to be specified occur at the surface S_1, which is a complicated free boundary, determined by simultaneously requiring $A(S_1) = 0$ and $\mathbf{n} \cdot \nabla A(S_1) = 0$. This is a very difficult calculation. To simplify the analysis S_1 is approximated by S_a as shown in Fig. 5, corresponding to the assumption that the equilibrium magnetic field is one dimensional, penetrating the same distance into the superconductor and stabilizer as determined by the critical state model. Thus, at equilibrium $w = B_0/\mu_0 J(T_0)$. The boundary conditions at S_a are given by

$$\begin{aligned} [\![T]\!]_{S_a} = [\![\partial T/\partial x]\!]_{S_a} &= 0 \\ A_1(S_a) &= 0 \\ \frac{\partial A_1}{\partial x}(S_a) &= 0 \ . \end{aligned} \tag{16}$$

In this approximation the tendency for the field to "bulge out" in the stabilizer region is ignored as well as the small surface current that develops on the superconductor-stabilizer

interface. The shape S_a greatly simplifies the stability analysis, allowing us to easily calculate how w moves during a period of flux penetration. Note also that region 3 has now been subdivided into two sections for convenience.

Under these assumptions, the equilibrium solution is given by

$$T_1 = T_2 = T_3 = T_4 \equiv T_0$$

$$A_2 = A_4 = 0 \tag{17}$$

$$A_1 = A_3 = -\frac{B_0}{2w}(x-w)^2$$

$T_0 < T_c$ represents the operating temperature of the superconductor.

General linearized equations

The stability of the tape is analyzed by determining the linearized conditions for the exponential growth of perturbations about the equilibrium solution just described. All quantities are expanded as

$$Q(x,y,t) = Q_0 + \tilde{Q}(x,y)e^{\gamma t} \tag{18}$$

where Q_0 represents the equilibrium value, $\tilde{Q}$ represents perturbation ($\tilde{Q}/Q_0 \ll 1$), and γ is the linear growth rate. Substituting into the basic equations and linearizing yields a set of equations for the perturbed quantities in each region

$$\begin{aligned}
&\text{Region 1} \left\{ \begin{array}{c} \gamma C\tilde{T}_1 = \kappa\nabla^2\tilde{T}_1 - \gamma J_0\tilde{A}_1 \\ \nabla^2\tilde{A}_1 = (\mu_0 J_c/T_c)\tilde{T}_1 \end{array} \right. \\
&\text{Region 2} \left\{ \begin{array}{c} \gamma C\tilde{T}_2 = \kappa\nabla^2\tilde{T}_2 \\ \tilde{A}_2 = 0 \end{array} \right. \\
&\text{Region 3} \left\{ \begin{array}{c} \gamma\hat{C}\tilde{T}_3 = \hat{\kappa}\nabla^2\tilde{T}_3 \\ \gamma\mu_0\tilde{A}_3 = \hat{\eta}\nabla^2\tilde{A}_3 \end{array} \right. \\
&\text{Region 4} \left\{ \begin{array}{c} \gamma\hat{C}\tilde{T}_4 = \hat{\kappa}\nabla^2\tilde{T}_4 \\ \gamma\mu_0\tilde{A}_4 = \hat{\eta}\nabla^2\tilde{A}_4 \end{array} \right.
\end{aligned} \tag{19}$$

Here, C and $\hat{C}$ are the superconductor and stabilizer specific heats, $\hat{\eta}$ is the stabilizer resistivity, and $J_0 = J_c(1 - T_0/T_c)$. In region 1 it has been assumed that $\tilde{T}_1$ is positive everywhere when linearizing $J(T)$. For $\tilde{T}_1 < 0$, Eq. (6) implies that $\tilde{J}_1 = 0$.

Nature of the solutions

Insight into the nature of the solutions for γ can be obtained by multiplying each equation by its respective complex conjugate variable. After integrating and manipulating algebraically, one obtains the quadratic relation

$$A\gamma^2 + B\gamma + C = 0 \tag{20}$$

where

$$\begin{aligned} A &= \frac{T_0}{\eta} \sum_{j=3}^{4} \int |\tilde{A}_j|^2 dS_j \\ B &= \sum_{j=1}^{4} \int \left[C_j |\tilde{T}_j|^2 + \frac{(T_c - T_0)}{\mu_0} |\nabla \tilde{A}_j|^2 \right] dS_j + \int J_0 (\tilde{A}_1 \tilde{T}_1^* + \tilde{A}_1^* \tilde{T}_1) dS_1 \\ C &= \sum_{j=1}^{4} \int \kappa_j |\nabla \tilde{T}_j|^2 dS_j \end{aligned} \tag{21}$$

and the subscript j denotes the different regions of the problem. Observe that (1) the coefficients A, B, and C are all real, (2) A and C are positive definitive, and (3) only the last term in B can be negative. The nature of the stability transition can be understood by considering the behavior of γ as a function of B or equivalently J_0.

Since Eq. (20) is quadratic in γ, the solutions are

$$\gamma = \frac{1}{2A} \left[-B \pm (B^2 - 4AC)^{1/2} \right] . \tag{22}$$

Figure 6 illustrates the solution in the complex γ plane. When $J_0 = 0$, then $B > 0$ and there are two stable roots. As J_0 increases, B decreases but still remains positive. When $B^2 = 4AC$, $B > 0$, the roots divide into a pair of complex conjugates with $Re(\gamma) < 0$. The

system is still stable. As J_0 further increases, B eventually equals zero. At this point γ has two purely imaginary roots and $Re(\gamma)$=0. Additional increases in J_0 cause B to become negative. The roots again occur as complex conjugates, although now $Re(\gamma) > 0$. As J_0 continues to increase, B continues to decrease, and the roots merge when $B^2 = 4AC$, $B < 0$, after which there are two real roots for γ with $Re(\gamma) > 0$.

Because of the asymmetric behavior of $J(T)$ about T_0, the true marginal stability point occurs when $B^2 = 4AC$, $B < 0$ as indicated in Fig. 6. The complex roots with $Re(\gamma) > 0$ are not actually unstable for the following reason. A mode with $Re(\gamma) > 0$, $Im(\gamma) \neq 0$, is oscillatory as well as growing and thus generates a $\tilde{T}_1$ which is positive part of the time and negative other times. However, whenever $\tilde{T}_1 < 0$, then as previously discussed, $\tilde{J}_1 = 0$ thereby modifying the coefficient B; in particular, the destabilizing term vanishes. We have attempted to find solutions to the linearized equations including alternating regions of positive and negative $\tilde{T}_1$, with the corresponding values of $\tilde{J}_1 = -(J_c/T_c)\tilde{T}_1$ or $\tilde{J}_1 = 0$. In no case did we find an eigenmode with $Re(\gamma) > 0$.

Case 1: the unstabilized, one dimensional tape

The simplest and most unstable geometry to analyze is a one dimensional, unstabilized tape. The external magnetic field is normal to the tape and penetrates into the superconductor as shown in Fig. 7. One now has $S_3 = S_4 = 0$ so the coefficient $A = 0$ and the solutions for the growth rate reduce to $\gamma = -C/B$. γ is always purely real and the transition from stable to unstable occurs as $B \to 0$ with γ switching from $-\infty$ to $+\infty$. There is no "normal" point of marginal stability through $\gamma = 0$. The linearized unstable growth rate is infinite at the transition. This divergence is resolved shortly by a nonlinear theory.

For case 1, Eq. (19) simplifies to

$$\frac{d^2\tilde{A}_1}{dx^2} = \frac{\mu_0 J_c}{T_c}\tilde{T}_1$$
$$\kappa\frac{d^2\tilde{T}_1}{dx^2} = \gamma C\tilde{T}_1 + \gamma J_0\tilde{A}_1 \qquad (23)$$

$$\kappa \frac{d^2 \tilde{T}_2}{dx^2} = \gamma C \tilde{T}_2$$

The problem is simplified by converting to dimensionless parameters. By substituting $\rho = x/w_0$, $U_1 = \tilde{T}_1/T_c$, $U_2 = \tilde{T}_2/T_c$, $\psi_1 = \tilde{A}_1/\mu_0 w_0^2 J_c$ and introducing $\Gamma = \gamma w_0^2 C/\kappa$, $\lambda = w/w_0 = B_0/\mu_0 J_0 w_0$, $\alpha = \mu_0 w_0^2 J_0 J_c / C T_c$, the eigenvalue problem can be written as

$$\begin{aligned} \frac{d^2\psi_1}{d\rho^2} &= U_1 \\ \frac{d^2 U_1}{d\rho^2} &= \Gamma U_1 + \alpha \Gamma \psi_1 \\ \frac{d^2 U_2}{d\rho^2} &= \Gamma U_2 \end{aligned} \tag{24}$$

subject to

$$\begin{aligned} & U_2'(1) = 0 \\ & \psi_1(\lambda) = U_1'(\lambda)/U_1(\lambda) - U_2'(\lambda)/U_2(\lambda) = 0 \\ & \psi_1'(0) = U_1(0) = 0 \ . \end{aligned} \tag{25}$$

Equation (25) accounts for all boundary conditions except $\partial A_1(S_a)/\partial\rho = 0$. Linearization of this condition describes how the free boundary w moves under the perturbation; that is writing $S_a = w + \delta w$ yields $\delta w/w_0 = \psi_1'(\lambda)/(1 - T_0/T_c)$.

The eigenvalue problem for Γ can be solved in a straightforward manner. First, the solution in region 2 is easily found and is given by

$$U_2 = U_{20} \cosh[\Gamma^{1/2}(1-\rho)] \tag{26}$$

which implies that

$$\frac{U_2'(\lambda)}{U_2(\lambda)} = -\Gamma^{1/2} \tanh[\Gamma^{1/2}(1-\lambda)] \ . \tag{27}$$

The solutions in region 1 can be written as

$$\psi_1 = \sum_{j=1}^{4} c_j \exp(k_j \rho)$$
$$U_1 = \sum_{j=1}^{4} c_j k_j^2 \exp(k_j \rho) \tag{28}$$

where $k_1 = -k_2 \equiv K$, $k_3 = -k_4 \equiv iH$ and

$$K^2 = \frac{\Gamma}{2} + \frac{1}{2}(\Gamma^2 + 4\alpha\Gamma)^{1/2}$$
$$H^2 = -\frac{\Gamma}{2} + \frac{1}{2}(\Gamma^2 + 4\alpha\Gamma)^{1/2} \ . \tag{29}$$

The c_j are unknown coefficients. Applying the boundary conditions on U_1 and ψ_1 from Eq. (25) leads to a set of four linear homogeneous algebraic equations for the c_j. Setting the determinant to zero gives the following, somewhat complicated dispersion relation for Γ.

$$\frac{2\alpha\Gamma + (\Gamma^2 + 2\alpha\Gamma)\cosh K\lambda \cos H\lambda + \alpha^{1/2}\Gamma^{3/2} \sinh K\lambda \sin H\lambda}{(H^2 + K^2)(H \cosh K\lambda \sin H\lambda + K \sinh K\lambda \cos H\lambda)} = -\Gamma^{1/2} \tanh[\Gamma^{1/2}(1-\lambda)] \ . \tag{30}$$

The stability threshold can be determined by noting that (from the definition of H) $\Gamma = H^4/(\alpha - H^2)$. Thus, instability only occurs when $0 < H^2 < \alpha$. Next, recall that the stability transition occurs through $\Gamma \to \infty$ implying that $\alpha \approx H^2$ and $K \to \infty$. In this region of parameter space the dispersion relation reduces to

$$\Gamma^{1/2} \approx -\alpha^{1/2} \tan(\alpha^{1/2}\lambda) \ . \tag{31}$$

The condition for stability is given by

$$\alpha^{1/2}\lambda < \pi/2 \tag{32}$$

or in terms of the physical variables

$$B_0^2 < \frac{\pi^2}{4}\mu_0 C(T_c - T_0) \ . \tag{33}$$

This result is identical to adiabatic limit first derived by Swartz and Bean.[2] Observe that without a stabilizer, only a small magnetic field is required to drive the instability. For instance, for NbTi with $C = 5.5 \times 10^3$ J/m^3 K, $T_c = 6.5$ K, then $B_0 \approx 0.2$T. In physical units, the characteristic growth rate is of the order

$$\gamma \sim \frac{\mu_0 \kappa J_c^2 (T_c - T_0)}{C^2 T_c^2} \ . \tag{34}$$

For typical parameters $\kappa = 0.1$ W/m K and $J_c = 1.5 \times 10^9$ A/m^2, then $\gamma \sim 510$ (sec)$^{-1}$, a very fast growth rate indeed.

The last point of interest is the eigenfunctions which are illustrated in Fig. 8. Note that all of the eigenfunctions are smooth and satisfy the boundary conditions. Also, as required, the function $U_1(\rho)$ is always positive.

Nonlinear solution

While the linearized analysis leads to many physically intuitive results, its main weakness is the prediction of infinite growth rates at the stability transition. This question is addressed by means of a nonlinear solution obtained by variational techniques.

An examination of the basic model indicates that there are two important nonlinear effects to consider. First there is the $\tilde{J}\tilde{E}$ contribution to the main instability drive. Heuristically, the electric power generated by flux penetration can be written iteratively as

$$JE \approx -\gamma J_0 \tilde{A} \left(1 - \frac{U_1 e^{\gamma t}}{1 - T_0/T_c} \right) \ . \tag{35}$$

Note that as $\gamma \to \infty$, the "small" nonlinear term grows infinitely fast and, since $U_1 > 0$, is in the direction to oppose the main destabilizing drive. In other words, as the temperature increases due to the instability, the current $J(T)$ decreases nonlinearly, producing a stabilizing effect.

The second important nonlinear effect is the time dependence of the penetration depth. As the instability grows the boundary between regions 1 and 2 moves such that

$w \to w_0$; that is as $J(T)$ decreases a wider current carrying region is required to shield the same magnetic field. This additional penetration produces further heating, representing a nonlinear destabilizing effect.

Both of these effects are included in the analysis presented below. The nonlinear equations in region 1 have the form

$$C\frac{\partial T_1}{\partial t} = \kappa\frac{\partial^2 T_1}{\partial x^2} - J_c\frac{\partial A_1}{\partial t}\left(1 - \frac{T_1}{T_c}\right)$$
$$\frac{\partial^2 A_1}{\partial x^2} = -\mu_0 J_c\left(1 - \frac{T_1}{T_c}\right) . \tag{36}$$

Introducing normalized variables, $T_1 = T_0 + (T_c - T_0)U$, $A_1 = (\mu_0 J_0 \overline{w}^2)\psi$, $x = \overline{w}\rho$, and $t = (\overline{w}^2 C/\kappa)\tau$ leads to

$$\frac{\partial U}{\partial \tau} = \frac{\partial^2 U}{\partial \rho^2} - \alpha\lambda^2(1-U)\frac{\partial \psi}{\partial \tau}$$
$$\frac{\partial^2 \psi}{\partial \rho^2} = -(1-U) \tag{37}$$

where $\overline{w} = B_0/\mu_0 J_0$ and $\alpha\lambda^2 = \mu_0 \overline{w} J_0 J_c/CT_c$ as in the linear case. The boundary conditions are given by

$$U(0,\tau) = \frac{\partial \psi}{\partial \rho}(0,\tau) - 1 = 0$$
$$U(s,\tau) = \psi(s,\tau) = \frac{\partial \psi}{\partial \rho}(s,\tau) = 0 . \tag{38}$$

Here, $s(\tau) = w(\tau)/\overline{w}$ represents the moving interface between regions 1 and 2. Initially $s(0) = 1$. Note also that $U(s,\tau)$ has been set to zero rather than matching onto a region 2 solution. In the limit of rapid growth this is a good approximation, introduced here primarily for simplicity.

Equation (37) can be cast in the form of a pair of variational principles for U and ψ and solved using trial functions. The variational forms are

$$L_U = \int_0^s d\rho \left[U\frac{\partial \hat{U}}{\partial \tau} + \frac{1}{2}\left(\frac{\partial U}{\partial \rho}\right)^2 - \alpha\lambda^2\frac{\partial \hat{\psi}}{\partial \tau}(U^2 - 2U)\right]$$
$$L_\psi = \int_0^s d\rho \left[\frac{1}{2}\left(\frac{\partial \psi}{\partial \rho}\right)^2 - \psi(1-\hat{U})\right] + \psi(0,\tau) \tag{39}$$

where $\hat{U}$ and $\hat{\psi}$ are held fixed during the variation. Once the variation is taken, then $\hat{U}$ and $\hat{\psi}$ are set to U and ψ respectively. After carefully considering the boundary conditions and differential equations, we choose the following trial functions for U and ψ

$$\begin{aligned} U &= \overline{U}(z - z^2) \\ \psi &= \frac{1}{2}\left[-s + 2sz - s^2z^2 + 2(s^2 - s)z^3 - (s^2 - s)z^4\right] . \end{aligned} \tag{40}$$

Here, the substitution $\rho = sz$ has been made. The functions $\overline{U}(\tau)$ and $s(\tau)$ are the unknown time dependent variational functions.

Equation (40) is substituted into Eq. (39). The equations determining $\overline{U}$ and s are obtained by setting

$$\begin{aligned} \frac{\partial L_U}{\partial \overline{U}} &= 0 \\ \frac{\partial L_\psi}{\partial s} &= 0 . \end{aligned} \tag{41}$$

After some algebra one obtains a single equation for $V(\tau) \equiv \overline{U}(\tau)/6$ given by

$$[1 - \alpha\lambda^2 f(V)]\frac{dV}{d\tau} = -Vg(V) \tag{42}$$

where

$$\begin{aligned} g(V) &= \frac{20(1-V)^3}{2-V} \\ f(V) &= \frac{13}{21}\frac{[1 - V/(1+\sqrt{3}/9)][1 - V/(1-\sqrt{3}/9)]}{(1-V)^2(2-V)} . \end{aligned} \tag{43}$$

In the analysis, the superconductor is considered unstable if the temperature anywhere reaches the value T_c. From Eq. (40), it follows that the maximum temperature occurs when $z = 1/2$ (i.e. $x = w/2$). In terms of V, $T_{max} = T_c$ when $V = 2/3$. The goal now is to solve Eq. (42) to determine under what conditions, and how long it takes, for $V(\tau)$ to reach the value $2/3$.

Consider first the linear regime $V \ll 1$. Equation (42) reduces to

$$(1 - \frac{13\alpha\lambda^2}{42})\frac{dV}{d\tau} \approx -10V \tag{44}$$

which has as its solution $V = V_0 \exp(\Gamma\tau)$ where

$$\Gamma = \frac{32.3}{\alpha\lambda^2 - 3.23} \,. \tag{45}$$

As in the exact linear case the stability transition occurs through $\Gamma \to \infty$. The critical $\alpha\lambda^2$ has the value $\alpha\lambda^2 = 42/13 \approx 3.23$, which should be compared with the exact value given by Eq. (32), $\alpha\lambda^2 = \pi^2/4 = 2.48$. This difference is a consequence of substituting trial functions rather than the exact form of the eigenfunction and using slightly different boundary conditions at the region 1-2 interface.

It is now of interest to set $\alpha\lambda^2 = 42/13$ in the nonlinear case to determine how the linear solution with infinite growth evolves nonlinearly. Choosing this value for $\alpha\lambda^2$, we find that the equation for V reduces to

$$\frac{dV}{d\tau} = \frac{260(1-V)^5}{13V^2 - 25V + 11} \,. \tag{46}$$

Observe that in contrast to the linear theory, $V(\tau)$ is well behaved even for small amplitudes; there is no infinite growth. A numerically computed solution is illustrated in Fig. 9 where we see that V increases monotonically in time reaching the critical value $V = 2/3$ at $\tau = 0.09$. At this time the superconductor goes normal.

Case 2: two dimensional tape with perfect stabilizer

The one dimensional unstabilized tape represents the most unstable system and provides a lower bound to the stable parameter space. An upper bound is obtained by considering a two dimensional tape in contact with an ideal perfectly conducting stabilizer ($\hat{\eta} = 0, \hat{\kappa} = \infty$). Using the same normalization associated with Eq. (24), the governing linearized equations have the form

$$\begin{aligned} \nabla^2 U_1 &= \Gamma U_1 + \alpha\Gamma\psi_1 \\ \nabla^2 \psi_1 &= U_1 \\ \nabla^2 U_2 &= \Gamma U_2 \end{aligned} \tag{47}$$

where $\nabla^2 = \partial^2/\partial\rho^2 + \partial^2/\partial\zeta^2$ and $\rho = x/w_0, \zeta = y/w_0$.

In the stabilizer $U_3 = U_4 = \psi_3 = \psi_4 = 0$ because of the assumptions of infinite thermal and electrical conductivity. The effect of the stabilizer enters only through the boundary conditions, which are summarized below

$$\begin{aligned} U_1(0,\zeta) &= \frac{\partial\psi_1}{\partial\rho}(0,\zeta) = 0 \\ U_1(\rho,\epsilon) &= U_2(\rho,\epsilon) = \psi_1(\rho,\epsilon) = 0 \\ \frac{\partial U_2}{\partial\rho}(w_0,\zeta) &= 0 \\ \frac{\partial U_1}{\partial\zeta}(\rho,0) &= \frac{\partial U_2}{\partial\zeta}(\rho,0) = \frac{\partial\psi_1}{\partial\zeta}(\rho,0) = 0 \\ \psi_1(\lambda,\zeta) &= [\![\frac{\partial U}{\partial\rho}/U]\!]_\lambda = 0 \,. \end{aligned} \tag{48}$$

Here $\epsilon = d/w_0$ is the dimensionless superconductor thickness. The dominant effect of the stabilizer is to force the perturbed temperature and flux to be zero along the stabilizer-superconductor interface $\zeta = \epsilon$ (i.e. $y = d$). In this simplified ideal model, the coefficient A appearing in Eq. (21) vanishes indicating that only real solutions for Γ are possible and that the stability transition occurs through $\Gamma \to \infty$.

The solution to Eq. (47) can be found by separation of variables:

$$\begin{aligned} \psi_1(\rho,\zeta) &= \psi_1(\rho)\cos(k_y\zeta) \\ U_1(\rho,\zeta) &= U_1(\rho)\cos(k_y\zeta) \\ U_2(\rho,\zeta) &= U_{20}\cosh[k_x(1-\rho)]\cos(k_y\zeta) \end{aligned} \tag{49}$$

where $k_y^2 = (\pi/2\epsilon)^2$ and $k_x^2 = (\pi/2\epsilon)^2 + \Gamma$. Substituting into Eq. (47) yields a set of one dimensional equations for the functions $U_1(\rho)$ and $\psi_1(\rho)$

$$\begin{aligned} \frac{d^2U_1}{d\rho^2} - k_x^2U_1 - \alpha\Gamma\psi_1 &= 0 \\ \frac{d^2\psi_1}{d\rho^2} - k_y^2\psi_1 - U_1 &= 0 \end{aligned} \tag{50}$$

subject to

$$\begin{aligned} U_1(0) = \frac{d\psi_1}{d\rho}(0) &= 0 \\ \psi_1(\lambda) = \frac{dU_1}{d\rho}(\lambda)\,/U_1(\lambda) + k_x\tanh[k_x(1-\lambda)] &= 0 \,. \end{aligned} \tag{51}$$

As in case 1, this is a fourth order system whose solutions can be written as

$$\psi_1 = \sum_{j=1}^{4} c_j \exp(k_j \rho)$$

$$U_1 = \sum_{j=1}^{4} c_j (k_j^2 - k_y^2) \exp(k_j \rho) \tag{52}$$

where $k_1 = -k_2 \equiv K, k_3 = -k_4 \equiv iH$ and

$$K^2 = k_y^2 + \frac{\Gamma}{2} + \frac{1}{2}\left(\Gamma^2 + 4\alpha\Gamma\right)^{1/2}$$

$$H^2 = -k_y^2 - \frac{\Gamma}{2} + \frac{1}{2}(\Gamma^2 + 4\alpha\Gamma)^{1/2} \ , \tag{53}$$

Applying the boundary conditions and setting the resultant determinant to zero yields the following dispersion relation

$$\frac{2\alpha\Gamma KH + (\Gamma^2 + 2\alpha\Gamma)KH \cosh K\lambda \cos H\lambda + \alpha\Gamma(\Gamma + 2k_y^2) \sinh K\lambda \sin H\lambda}{(K^2 + H^2)[K(H^2 + k_y^2) \cosh K\lambda \sin H\lambda + H(K^2 - k_y^2) \sinh K\lambda \cos H\lambda]} \tag{54}$$

$$= -k_x \tanh[k_x(1 - \lambda)] \ .$$

As expected, this complicated expression reduces to the dispersion relation for case 1 when $k_y^2 \to 0$.

If one again considers the transition region where $\Gamma \to \infty$, then Eq. (54) reduces to the following simple expression for Γ

$$\Gamma^{1/2} \approx -\frac{\alpha}{H_\infty} \tan H_\infty \lambda \tag{55}$$

where $H_\infty^2 = \alpha - k_y^2$. The condition for stability can be written as

$$\alpha^{1/2}\lambda < \frac{\pi}{2}\left(1 + \frac{w^2}{d^2}\right)^{1/2} \tag{56}$$

which should be compared to Eq. (32). Since $d \ll w$ for most applications, Eq. (56) represents a much weaker restriction on α than case 1. The interpretation is clear. In case 1 the only path for heat generated by flux penetration to leave the system is by thermal conduction across the $x = 0$ boundary. This is a relatively weak effect and instability can

easily occur. In case 2, the stabilizer acts as a perfect heat sink. Thus, when $d \ll w$, there is a much shorter path available for heat to leave the superconductor and a much greater flux penetration can be tolerated.

Equation (56) can be expressed in terms of the physical variables as follows

$$\mu_0 J_0^2 \frac{d^2 w^2}{d^2 + w^2} < \frac{\pi^2}{4} C(T_c - T_0) \ . \tag{57}$$

In the interesting limit $d \ll w$, Eq. (57) simplifies to

$$\mu_0 J_0^2 d^2 < \frac{\pi^2}{4} C(T_c - T_0) \tag{58}$$

indicating, as expected, that low current density and a thin superconductor tape are desirable for stability. The dependence on $J_0^2 d^2$ is similar to the stability limit for a face cooled conductor.[3] By treating the stabilizer as a perfect conductor, it has effectively become an ideal coolant. Finally, the perturbations $U_1(\rho, \zeta)$ and $\psi_1(\rho, \zeta)$ are illustrated in Fig. 10. The contours display a strong two dimensional dependence and clearly satisfy the boundary conditions. Also, the perturbed temperature U_1 is positive everywhere as required.

The general two dimensional case

The general two dimensional case represents the most realistic stability treatment. Even after linearization, the problem remains quite complex because of the high order of the system and the two dimensional geometry. To obtain an analytical solution we introduce an asymptotic expansion based on the small parameter d/w, the ratio of thickness to width of the superconductor.

After careful consideration we introduce the following normalized quantities (somewhat different from the previous normalization) in order to clarify the nature of the expansion: $A_j = \mu_0 J_0 d^2 \psi_j$, $T_j = (T_c - T_0) U_j$, $x = w\rho$, $y = d\zeta = d + \hat{d} - \hat{d}\xi$, $\gamma = (\kappa / C d^2)\Gamma$, $\alpha = \mu_0 J_0^2 d^2 / C(T_c - T_0)$, $\delta = \mu_0 \kappa / \hat{\eta} C$, $\nu = \hat{C} w^2 \kappa / C d^2 \hat{\kappa}$, $\beta = \hat{d}^2 / d^2$, and $\epsilon = d^2 / w^2$. Note that two definitions have been introduced for y so that $0 < \zeta < 1$ in the superconductor,

$0 < \xi < 1$ in the stabilizer, and $\zeta = \xi = 1$ is the interface. The linearized equations can be rewritten as

$$\begin{aligned} L\psi_1 &= U_1 & \psi_2 &= 0 \\ LU_1 &= \Gamma U_1 + \alpha\Gamma\psi_1 & LU_2 &= \Gamma U_2 \\ \hat{L}\psi_3 &= \delta\beta\Gamma\psi_3 & \hat{L}\psi_4 &= \delta\beta\Gamma\psi_4 \\ \hat{L}U_3 &= \nu\epsilon\beta\Gamma U_3 & \hat{L}U_4 &= \nu\epsilon\beta\Gamma U_4 \end{aligned} \tag{60}$$

where L and $\hat{L}$ are the differential operators

$$\begin{aligned} L &\equiv \frac{\partial^2}{\partial\zeta^2} + \epsilon\frac{\partial^2}{\partial\rho^2} \\ \hat{L} &\equiv \frac{\partial^2}{\partial\xi^2} + \epsilon\beta\frac{\partial^2}{\partial\rho^2} \ . \end{aligned} \tag{61}$$

With this normalization we introduce the following asymptotic ordering $\psi_j \sim U_j \sim \Gamma \sim \alpha \sim \delta \sim \nu \sim \beta \sim 1$, motivated by substituting typical numerical values for α, δ, ν and β. Only the parameter ϵ is assumed small: $\epsilon \ll 1$.

We now proceed to solve Eq. (60) region by region by expanding all dependent variables as an asymptotic series in ϵ. Consider first region 2. The leading order solutions for ψ_2 and U_2 satisfying the boundary conditions at $\zeta = 0$ are given by

$$\begin{aligned} \psi_2(\rho,\zeta) &= 0 \\ U_2(\rho,\zeta) &= \overline{U}_2(\rho)\cosh(\Gamma^{1/2}\zeta) + \ldots \end{aligned} \tag{62}$$

Here $\overline{U}_2(\rho)$ is an arbitrary function. Similarly, in region 4 we obtain

$$\begin{aligned} \psi_4(\rho,\xi) &= \overline{\psi}_4(\rho)\cosh[(\delta\beta\Gamma)^{1/2}\xi] + \ldots \\ U_4(\rho,\xi) &= \overline{U}_4(\rho) + \epsilon\beta(\nu\Gamma\overline{U}_4 - \frac{d^2\overline{U}_4}{d\rho^2})\frac{\xi^2}{2} + \ldots \end{aligned} \tag{63}$$

Both ψ_4 and U_4 satisfy the boundary conditions at $\xi = 0$, and $\overline{U}_4(\rho)$, $\overline{\psi}_2(\rho)$ are arbitrary functions.

We next match the jump conditions across the interface between regions 2 and 4. The jump conditions for the flux yield

$$\overline{\psi}_4(\rho) = 0 \ . \tag{64}$$

The temperature jump conditions give

$$\begin{aligned}\overline{U}_2(\rho)\cosh\Gamma^{1/2} &= \overline{U}_4(\rho)\\ \overline{U}_2(\rho)\frac{\kappa\Gamma^{1/2}}{d}\sinh\Gamma^{1/2} &= -\frac{\hat{\kappa}\epsilon\beta}{\hat{d}}\left(\nu\Gamma\overline{U}_4 - \frac{d^2\overline{U}_4}{d\rho^2}\right)\ .\end{aligned} \tag{65}$$

Eliminating $\overline{U}_2$ leads to a differential equation for $\overline{U}_4$

$$\begin{aligned}\frac{d^2\overline{U}_4}{d\rho^2} - \hat{k}_\rho^2\overline{U}_4 &= 0\\ \hat{k}_\rho^2 &= \nu\Gamma\left(1 + \frac{C}{\hat{C}\beta^{1/2}}\frac{\tanh\Gamma^{1/2}}{\Gamma^{1/2}}\right)\ .\end{aligned} \tag{66}$$

The solution satisfying the boundary condition at the midplane $x = w_0$ has the form

$$\overline{U}_4(\rho) = \overline{U}_{40}\cosh[\hat{k}_\rho(\rho - w_0/w)] \tag{67}$$

where $\overline{U}_{40}$ is an arbitrary constant. These results can be combined to give proper boundary conditions across the interfaces separating regions 1 and 2 and regions 3 and 4

$$\begin{aligned}\psi_2(1,\zeta) &= \psi_4(1,\xi) = 0\\ \left[\frac{1}{U_2}\frac{\partial U_2}{\partial\rho}\right]_{\rho=1,\zeta} &= \left[\frac{1}{U_4}\frac{\partial U_4}{\partial\rho}\right]_{\rho=1,\xi} = -\hat{k}_\rho\tanh[\hat{k}_\rho(w_0/w - 1)]\ .\end{aligned} \tag{68}$$

Consider next the solution in regions 1 and 3. The solutions for ψ_3 and U_3 satisfying the boundary conditions at $\xi = 0$ are given by

$$\begin{aligned}\psi_3(\rho,\xi) &= \overline{\psi}_3(\rho)\cosh[(\delta\beta\Gamma)^{1/2}\xi] + \ldots\\ U_3(\rho,\xi) &= \overline{U}_3(\rho) + \epsilon\beta\left(\nu\Gamma\overline{U}_3 - \frac{d^2\overline{U}_3}{d\rho^2}\right)\xi^2 + \ldots\end{aligned} \tag{69}$$

where $\overline{\psi}_3(\rho)$ and $\overline{U}_3(\rho)$ are arbitrary functions.

The solutions for ψ_1 and U_1 are coupled. A short calculation yields

$$\begin{aligned}\psi_1(\rho,\zeta) &= \overline{F}_1(\rho)\cosh K\zeta + \overline{F}_2(\rho)\cos H\zeta + \ldots\\ U_1(\rho,\zeta) &= K^2\overline{F}_1(\rho)\cosh K\zeta - H^2\overline{F}_2(\rho)\cos H\zeta + \ldots\end{aligned} \tag{70}$$

Here $\overline{F}_1(\rho), \overline{F}_2(\rho)$ are free functions and

$$K^2 = \frac{\Gamma}{2} + \frac{1}{2}\left(\Gamma^2 + 4\alpha\Gamma\right)^{1/2}$$
$$H^2 = -\frac{\Gamma}{2} + \frac{1}{2}\left(\Gamma^2 + 4\alpha\Gamma\right)^{1/2} \tag{71}$$

ψ_1 and U_1 satisfy the boundary conditions at $\zeta = 0$. Matching the jump conditions on ψ and U across the region 1–3 interface leads to a set of four linear equations involving the quantities $\overline{F}_1$, $\overline{F}_2$, $\overline{\psi}_1$, $\overline{U}_3$ and $\overline{U}_3''$. After a straightforward calculation $\overline{F}_1$, $\overline{F}_2$ and $\overline{\psi}_1$ can be eliminated in terms of $\overline{U}_3$ and $\overline{U}_3''$. The end result is a differential equation for $\overline{U}_3$ which can be written as

$$\frac{d^2\overline{U}_3}{d\rho^2} + k_\rho^2\overline{U}_3 = 0 \tag{72}$$

where

$$k_\rho^2 = \nu\left(-\Gamma + \frac{C}{\beta^{1/2}\hat{C}}Z\right) \tag{73}$$
$$Z = \frac{HK(H^2+K^2)\tanh K\tan H + (\delta\Gamma)^{1/2}\tanh(\delta\beta\Gamma)^{1/2}(H^3\tan H - K^3\tanh K)}{HK(H\tanh K - K\tan H) + (H^2+K^2)(\delta\Gamma)^{1/2}\tanh(\delta\beta\Gamma)^{1/2}}.$$

The dispersion relation is obtained by solving Eq. (72) and then choosing Γ (i.e. k_ρ^2) so that the boundary conditions are satisfied at $\rho = 0$ and $\rho = 1$. The boundary conditions are somewhat subtle. By introducing the asymptotic expansion, the $\partial^2/\partial\rho^2$ term has been neglected in three of the four differential operators occurring in the region 1–3 solutions; the order of the system with respect to ρ has been reduced from eighth to second order. Thus, only two rather than eight boundary conditions can be applied, and it is crucial to determine which two are dominant. The fact that Eq. (72) is written in terms of $\overline{U}_3$ does not imply that the $\overline{U}_3$ boundary conditions are dominant. We could just as easily have eliminated variables in terms of any of the other unknowns.

To understand the nature of the problem assume that Eq. (72) is solved subject to the $\overline{U}_3$ boundary conditions: $\overline{U}_3'(0) = 0, \overline{U}_3'(1)/\overline{U}_3(1) = -\hat{k}_\rho\tanh[\hat{k}_\rho(w_0/w - 1)]$. The solution for $\overline{U}_3$ is sketched in Fig. 11a for the case $\Gamma \ll 1$. Also illustrated are the solutions for the other quantities along the interface $\zeta = \xi = 1$. The solid lines represent the solutions obtained by directly calculating the other quantities from $\overline{U}_3$. The dashed curves represent

the same quantities, modified only near the boundaries $\rho = 0$ and $\rho = 1$, in such a way as to satisfy the proper boundary conditions. Note that U_1 and ψ_1 exhibit large, unphysical jumps. Mathematically, this implies that the neglect of $\partial^2/\partial\rho^2$ terms in the solutions for U_1 and ψ_1 is a poor approximation for the $\overline{U}_3$ boundary conditions.

These considerations lead us to conclude that the $U_1(0,\zeta)$ and $\psi_1(1,\zeta)$ boundary conditions are dominant. In terms of $\overline{U}_3$ this requires $\overline{U}_3(0) = \overline{U}_3(1) = 0$. A sketch of these solutions is illustrated in Fig. 11b. Note that only small modifications to the asymptotic solution are required for each quantity to satisfy the appropriate boundary conditions. The implication is that for the boundary conditions $\overline{U}_3(0) = \overline{U}_3(1) = 0$, the $\partial^2/\partial\rho^2$ terms neglected are indeed small and the asymptotic solution represents a good approximation to the true solution.

A simple physical interpretation of the boundary conditions is as follows. The presence of the coolant at $x = 0$ and the shielding at $x = w$ make both of these points act as approximate heat sinks. Thus, we intuitively expect the most unstable temperature perturbations to be localized away from these points in order to make access to cooling most difficult. This is the behavior indicated by U_1 and U_3 in Fig. 11b.

Based on the above discussion we determine the dispersion relation by solving Eq. (72) subject to $\overline{U}_3(0) = \overline{U}_3(1) = 0$. The result is

$$k_\rho^2 = \pi^2 \tag{74}$$

where k_ρ^2 is the complicated expression given by Eq. (73).

The stability threshold can be obtained analytically by considering the interesting limit $\Gamma \to 0$ and $\delta < 1$. The condition $\Gamma \to 0$ appears to violate the discussion associated with Eq. (22) which implies that $\gamma = -B/2A$ is finite at the stability threshold $B^2 = 4AC, B < 0$. A careful dimensional analysis not presented here, shows that in terms of the normalized variables $\Gamma \sim \epsilon^2$ at this point. Because of the small ϵ expansion, the threshold in our analysis appears at $\Gamma = 0$ in leading order.

The condition $\delta < 1$, which is reasonably well satisfied for practical cases, is required to eliminate spurious roots from the dispersion relation. For typical parameters $\kappa =$

0.1W/mK, $\hat{\eta} = 2 \times 10^{-9}\Omega$m, and $C = 5.5 \times 10^3$ J/m^3 K, then $\delta \approx 0.01$. The quantity $\delta = \tau_{\hat{\eta}}/\tau_\kappa$ where $\tau_{\hat{\eta}}$ and τ_κ are the resistive diffusion time across the stabilizer and the thermal diffusion time across the superconductor respectively. For $\delta < 1$, the flux can diffuse "instantaneously" with respect to the flow of heat. This is consistent with the structure of the eigenfunctions in the stabilizer and superconductor, which connect smoothly across the interface. When $\delta > 1$, the stabilizer acts like a perfect electrical conductor and as flux penetrates the superconductor a surface current must develop across the interface. This regime requires a different set of boundary conditions than those imposed on the asymptotic solutions, much more closely related to case 2, the two dimensional tape with perfect stabilizer.

On the basis of this discussion, we introduce the assumptions $\Gamma \to 0$ and $\delta < 1$ into the dispersion relation. A short calculation yields

$$\Gamma \approx \Gamma_0 \left[\frac{3C}{\pi^2 \hat{C}} \left(\frac{\alpha\nu}{3\beta\delta - \beta^{1/2}\alpha} \right) - 1 \right]$$

$$\Gamma_0 = \pi^2 \left(\nu + \frac{2\pi^2}{3} + \frac{\nu C}{\beta^{1/2}\hat{C}} + \frac{2\pi^4}{15} \frac{\beta^{1/2}\hat{C}}{\nu C} \right)^{-1} . \tag{75}$$

Near marginal stability Γ is an increasing function of α. The condition for stability can be written as

$$\alpha \leq \frac{3\beta^{1/2}\delta}{1 + 3\nu C/\pi^2 \beta^{1/2}\hat{C}} \tag{76}$$

or in terms of the physical parameters

$$J_0^2 w^2 < \frac{\pi^2 \hat{\kappa}}{\hat{\eta}} \left(\frac{\hat{d}}{d} \right)^2 \frac{T_c - T_0}{1 + \pi^2 d\hat{d}\hat{\kappa}/3w^2\kappa} . \tag{77}$$

Equation (77) is the desired stability relation. If one takes the limit $d\hat{d}\hat{\kappa}/w^2\kappa \to 0$, then the second term in the denominator is negligible and the stability criterion reduces to

$$J_0^2 w^2 < \frac{\pi^2 \hat{\kappa}}{\hat{\eta}} \left(\frac{\hat{d}}{d} \right)^2 (T_c - T_0) . \tag{78}$$

This result is identical to the stability condition first derived by Hart[1] except for a numerical factor. The π^2 in Eq. (78) should be replaced by $\pi^2/4$ for equality. This discrepancy is presumably due to slightly different assumptions about the boundary conditions.

The additional term in the denominator of Eq. (77) represents a destabilizing effect; that is, the critical $J_0 w$ is lowered. Physically, the term represents the ratio of the thermal resistances across the height of the superconductor to that along the current carrying width w of the stabilizer. Even though $d \ll w$, the resistances can be comparable since $\hat{\kappa} \gg \kappa$.

To determine the importance of this term we plot in Fig. 12 curves of the critical $J_0 w$ vs w/d for various $\hat{d}/d$, assuming Nb_3Sn with $\hat{\kappa} = 10^2$W/m K, $\kappa = 10^{-1}$ W/m K, $T_c - T_0 = 14$ K, $\hat{\eta} = 2\times10^{-9}\Omega$m, and $C = 5.5\times10^3$J/m^3 K. Also plotted for comparison are the results for the idealized cases given by Eqs. (33) and (58). Note that when $w/d \lesssim 100$ the thermal diffusion in the superconductor can become important in the general case.

Discussion

The flux jump stability characteristics of a tape superconductor have been analyzed for several different cases: unstabilized superconductor, perfectly stabilized superconductor, and a full two dimensional stabilized superconductor with finite $\hat{\kappa}$ and $\hat{\eta}$ in the stabilizer. The stability boundaries for these cases, Eqs. (33), (58), and (77) can be written in a more uniform form useful for comparisons.

Unstabilized Tape:

$$\frac{\mu_0 J_0^2 w^2}{C(T_c - T_0)} < \frac{\pi^2}{4} \tag{79}$$

Perfectly Stabilized Tape:

$$\frac{\mu_0 J_0^2 w^2}{C(T_c - T_0)} < \frac{\pi^2}{4}\left(\frac{w}{d}\right)^2 \tag{80}$$

Two Dimensional Case:

$$\frac{\mu_0 J_0^2 w^2}{C(T_c - T_0)} < \pi^2 \frac{\hat{C}}{C}\left(\frac{w}{d}\right)^2 \frac{\tau_{\hat{\eta}}/\tau_{\hat{\kappa}}}{1 + R_\perp/R_\parallel} \,. \tag{81}$$

In Eq. (81) $\tau_{\hat{\eta}} = \mu_0 \hat{d}^2/\hat{\eta}$ and $\tau_{\hat{\kappa}} = \hat{C} w^2/\hat{\kappa}$ are the characteristic times for flux diffusion across the stabilizer and thermal diffusion along the stabilizer respectively. Similarly, $R_\perp = 2d/3\kappa w L$ and $R_\parallel = 2w/\pi^2 \hat{\kappa} \hat{d} L$ are the thermal resistivities across the superconductor and along the stabilizer respectively, with L the length of tape along the direction of

current flow. Since $\tau_{\hat{\eta}} < \tau_{\hat{\kappa}}$ for the cases under consideration, the two dimensional boundary lies intermediate to the two idealized cases. The analysis presented here shows that thermal conduction across the superconductor can play a significant destabilizing role for $w/d \lesssim (3\hat{d}\hat{\kappa}/d\kappa)^{1/2} \sim 100$.

Acknowledgements

One of the authors (JPF) would like to thank P. Rosenau of the Technion and T. Hsu of MIT for several extremely informative discussions during the course of the work.

The work performed by J. Schwartz was under appointment to the Magnetic Fusion Energy Technology Fellowship which is administered for the US Department of Energy by Oak Ridge Associated Universities.

References

1 **Hart, H. R. Jr.** Magnetic Instabilities and Solenoid Performance: Applications of the Critical State Model. Proceedings of the 1968 Summer Study on Superconducting Devices and Accelerators, Part II, BNL 50155 (C-55), (1968), 571, Brookhaven National Laboratory.

2 **Swartz, P. S. and Bean, C. P.** A Model for Magnetic Instabilities in Hard Superconductors: the Adiabatic Critical State. *Journal of Applied Physics* (1968) **39**, 4991.

3 **Ogasawara, T.** Feasibility Study on Large-Scale, High Current Density Superconductor by Dynamic Stabilization, Part 1: Magnetic Stability, *Cryogenics* (1987) **27**, 673.

4 **Wipf, S. L.** Magnetic Instabilities in Type II Superconductors, *Physics Review* (1967) **161(2)**, 404.

5 **Hancox, R.** Stability Against Flux Jumps in Nb_3Sn, *Physics Letters* (1965) **16**, 208.

6 **Duchateau, J. L. and Turck, B.** Theoretical and Experimental Study of Magnetic Instabilities in Multifilamentary Nb-Ti Superconducting Composites, IEEE Transactions on Magnetics (1975) **MAG-11**, 350.

7 **Kremlev, M. G.** Damping of Flux Jumping by Flux-flow Resistance, Cryogenics (1974), 132.

8 **Kremlev, M. G., Mints, R. G. and Rakhmanov, A. L.** Magnetic Instabilities in Superconducting Composites, *J. Phys. D: Appl. Phys.*, (1974) **10**, 1821.

9 **Wilson, M. N.** Superconducting Magnets, *Clarendon Press*, Oxford (1983) Chapter 7.

Figure captions

Fig. 1 Schematic diagram of (a) edge cooled and (b) face cooled superconducting tapes.

Fig. 2 Model of $J(T)$ for the superconductor.

Fig. 3 (a) Steady state current pattern in the actual superconductor-stabilizer system; (b) Simple approximation used in the analysis.

Fig. 4 Geometry determining the magnetic boundary condition. The total flux Φ is conserved during a perturbation.

Fig. 5 Multi-region geometry used for specifying the boundary conditions. Also shown is the approximate free boundary surface S_a.

Fig. 6 Trajectory of the roots of the dispersion relation in complex γ space as J_0 is increased.

Fig. 7 Unstabilized, one dimensional tape geometry, showing the equilibrium magnetic field.

Fig. 8 Normalized eigenfunctions for the unstabilized superconductor with $w/w_0 = 0.5$.

Fig. 9 $V(\tau)$ vs τ at the marginal stability point $\alpha\lambda^2 = 42/13$. The superconductor goes normal when $V = 2/3$.

Fig. 10a Contour plots of $U_1(\rho, \zeta)$.

Fig. 10b Contour plots of $\psi_1(\rho, \zeta)$ for the case $\alpha = 10^3$, $\lambda = 0.5$, $\Gamma \to \infty$.

Fig. 11 Sketch of $U_j(\rho, 1), \psi_j(\rho, 1)$ vs ρ for (a) the U_3 boundary conditions at $\rho = 0, 1$ dominant and (b) the U_1 and ψ_1 boundary conditions at $\rho = 0, 1$ dominant.

Fig. 12 Curves of critical $J_0 w$ vs w/d for various $\hat{d}/d$.

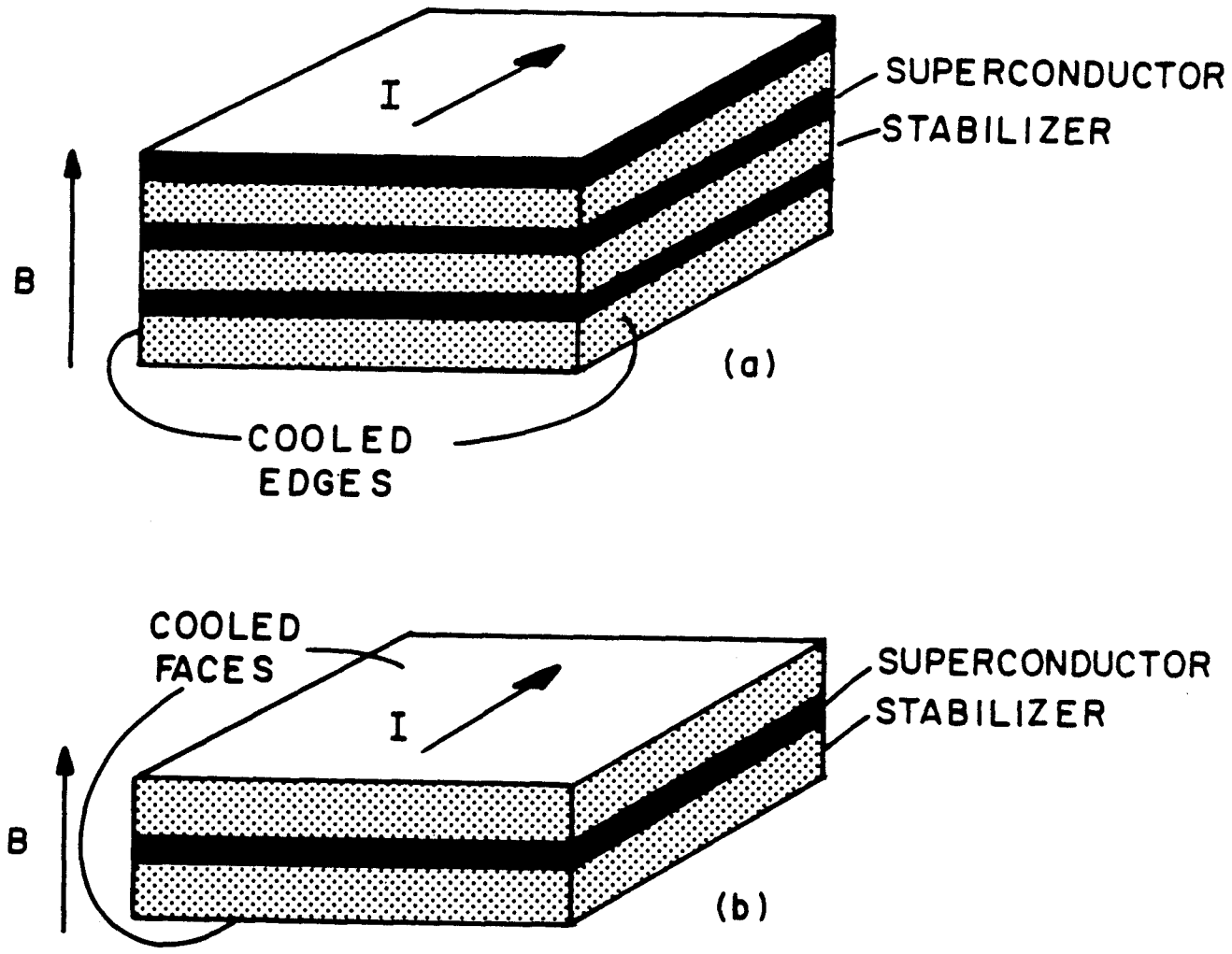

Fig. 1 Schematic diagram of (a) edge cooled and (b) face cooled superconducting tapes.

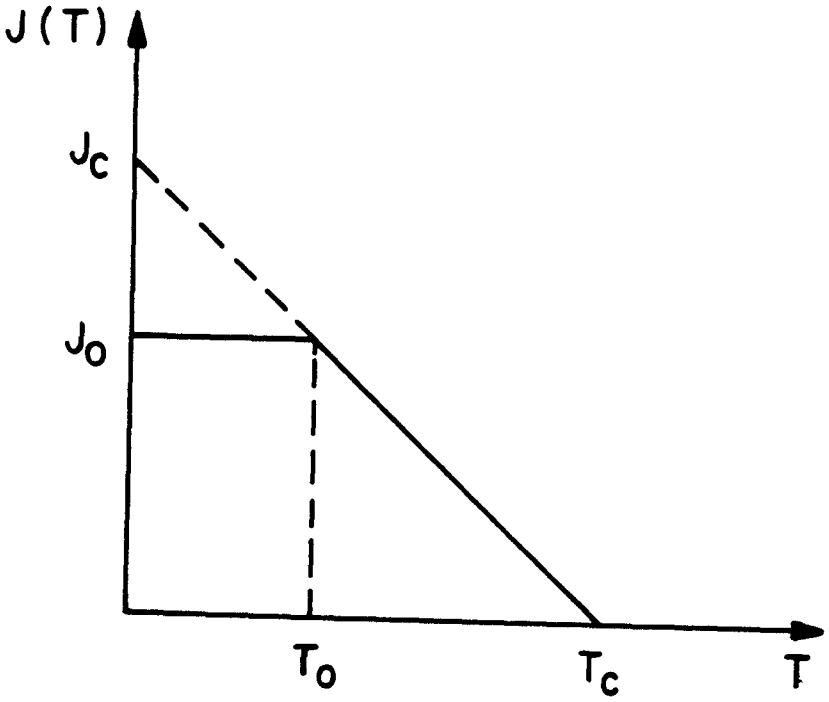

Fig. 2 Model of $J(T)$ for the superconductor.

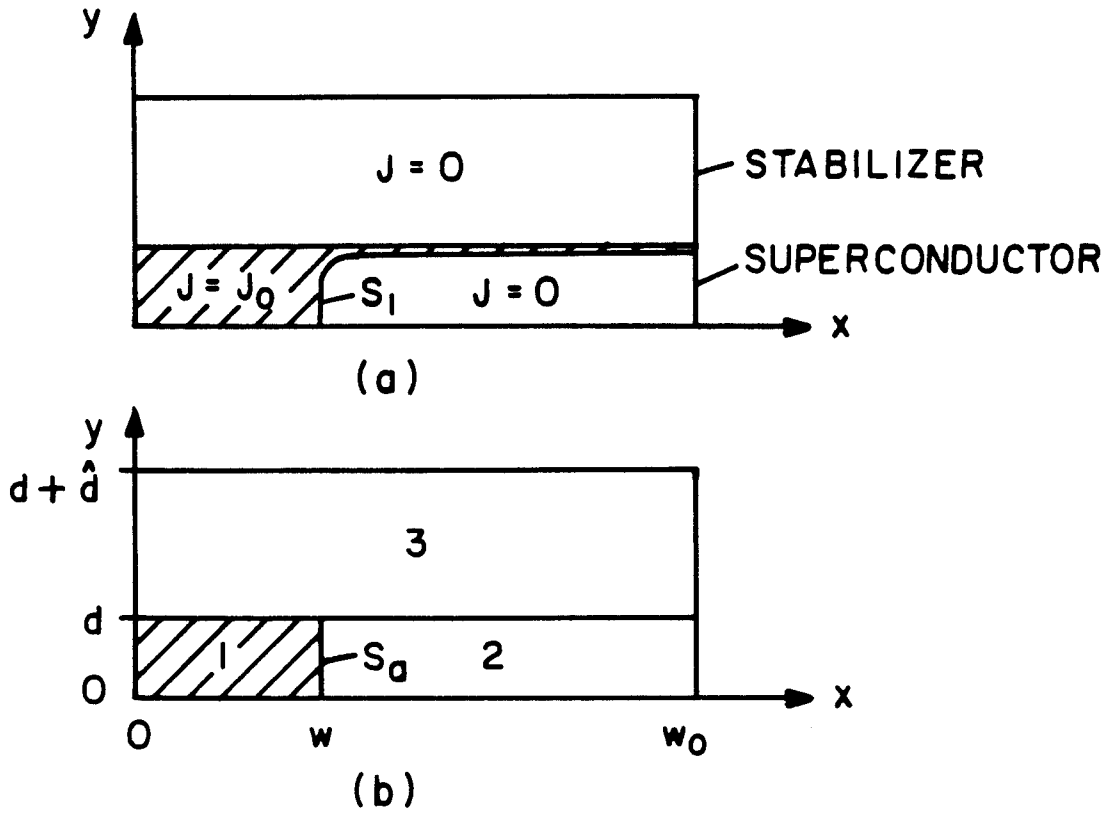

Fig. 3 (a) Steady state current pattern in the actual superconductor-stabilizer system; (b) Simple approximation used in the analysis.

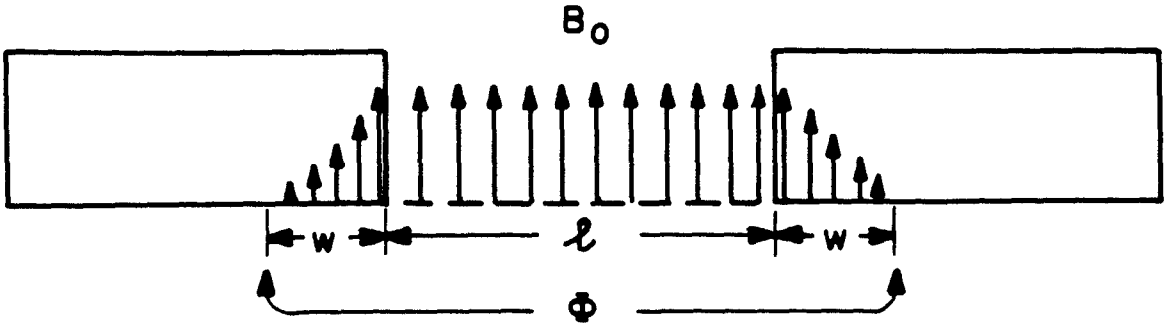

Fig. 4 Geometry determining the magnetic boundary condition. The total flux Φ is conserved during a perturbation.

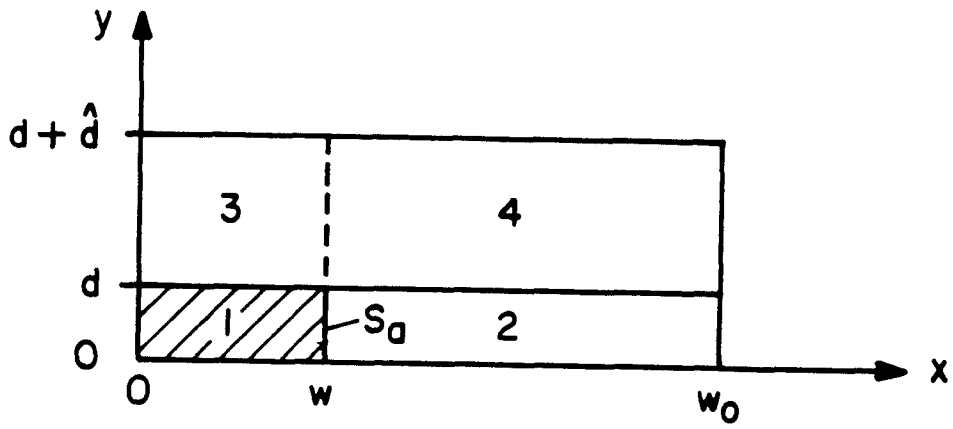

Fig. 5 Multi-region geometry used for specifying the boundary conditions. Also shown is the approximate free boundary surface S_a.

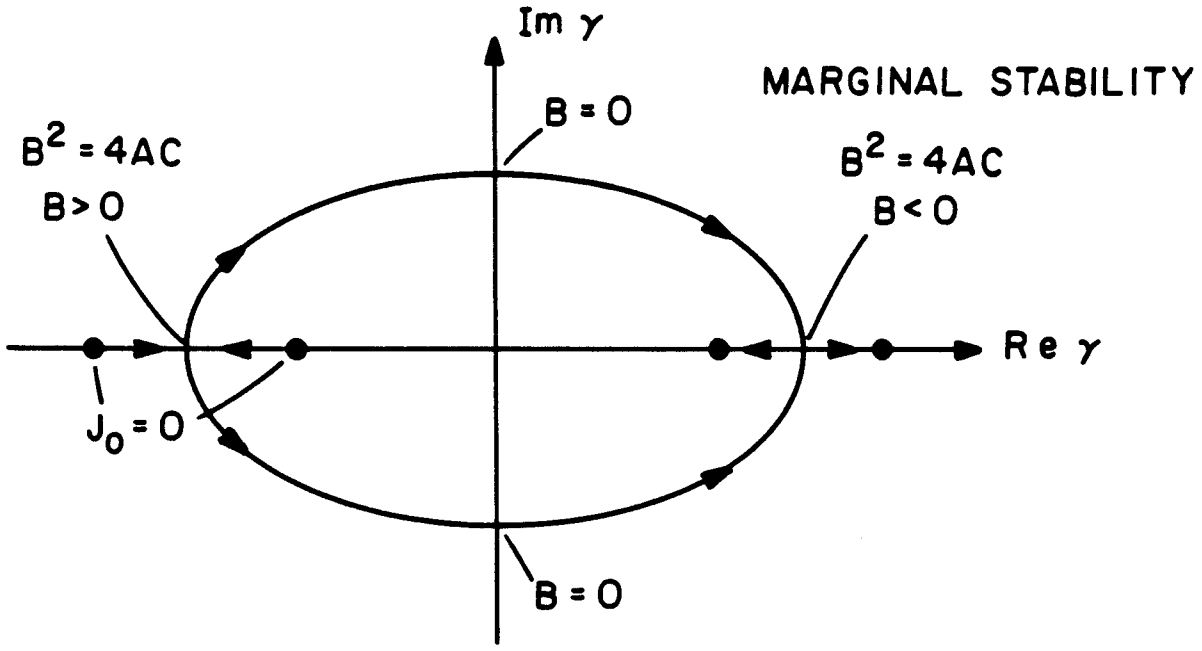

Fig. 6 Trajectory of the roots of the dispersion relation in complex γ space as J_0 is increased.

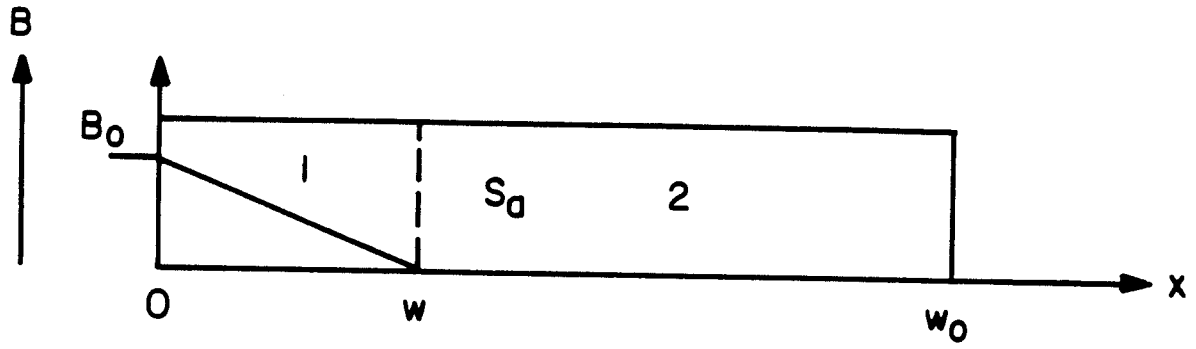

Fig. 7 Unstabilized, one dimensional tape geometry, showing the equilibrium magnetic field.

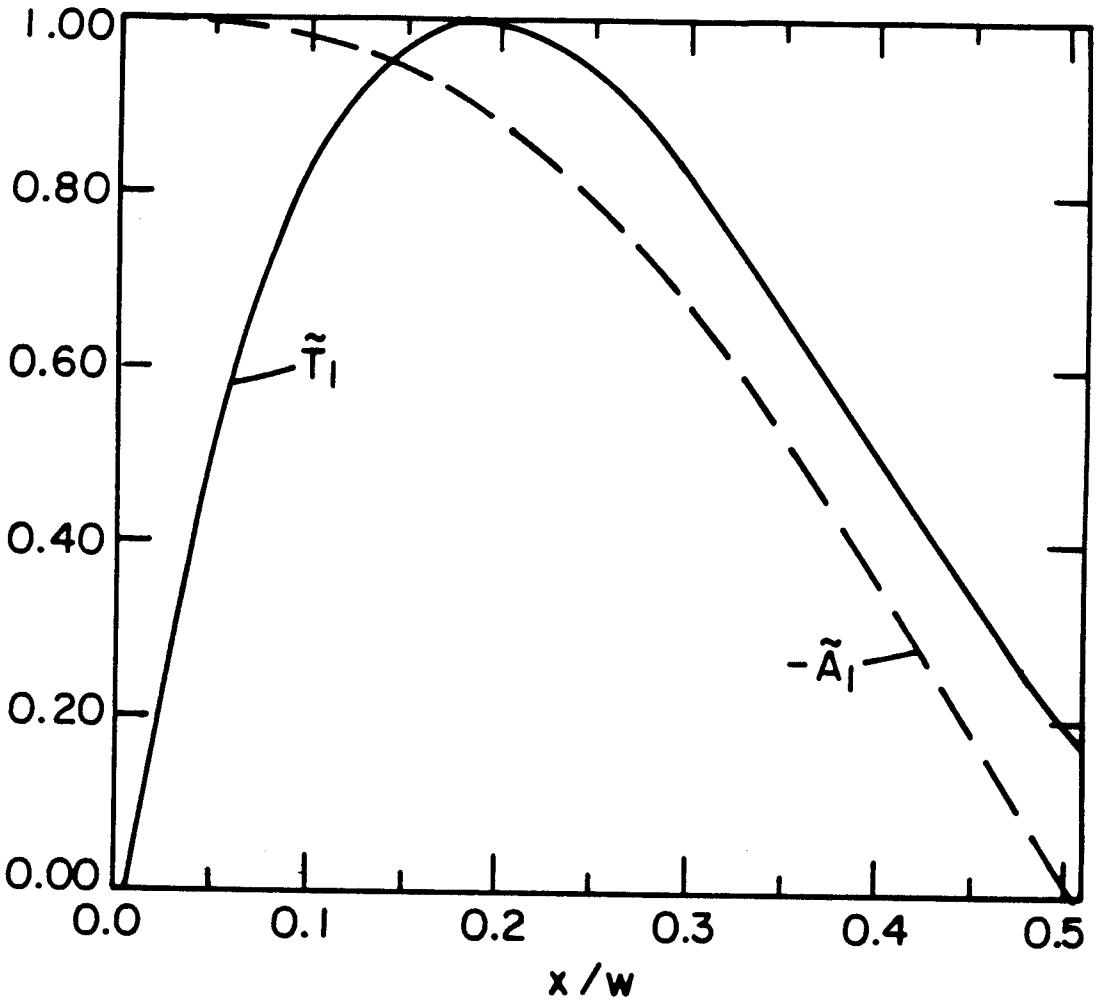

Fig. 8 Normalized eigenfunctions for the unstabilized superconductor with $w/w_0 = 0.5$.

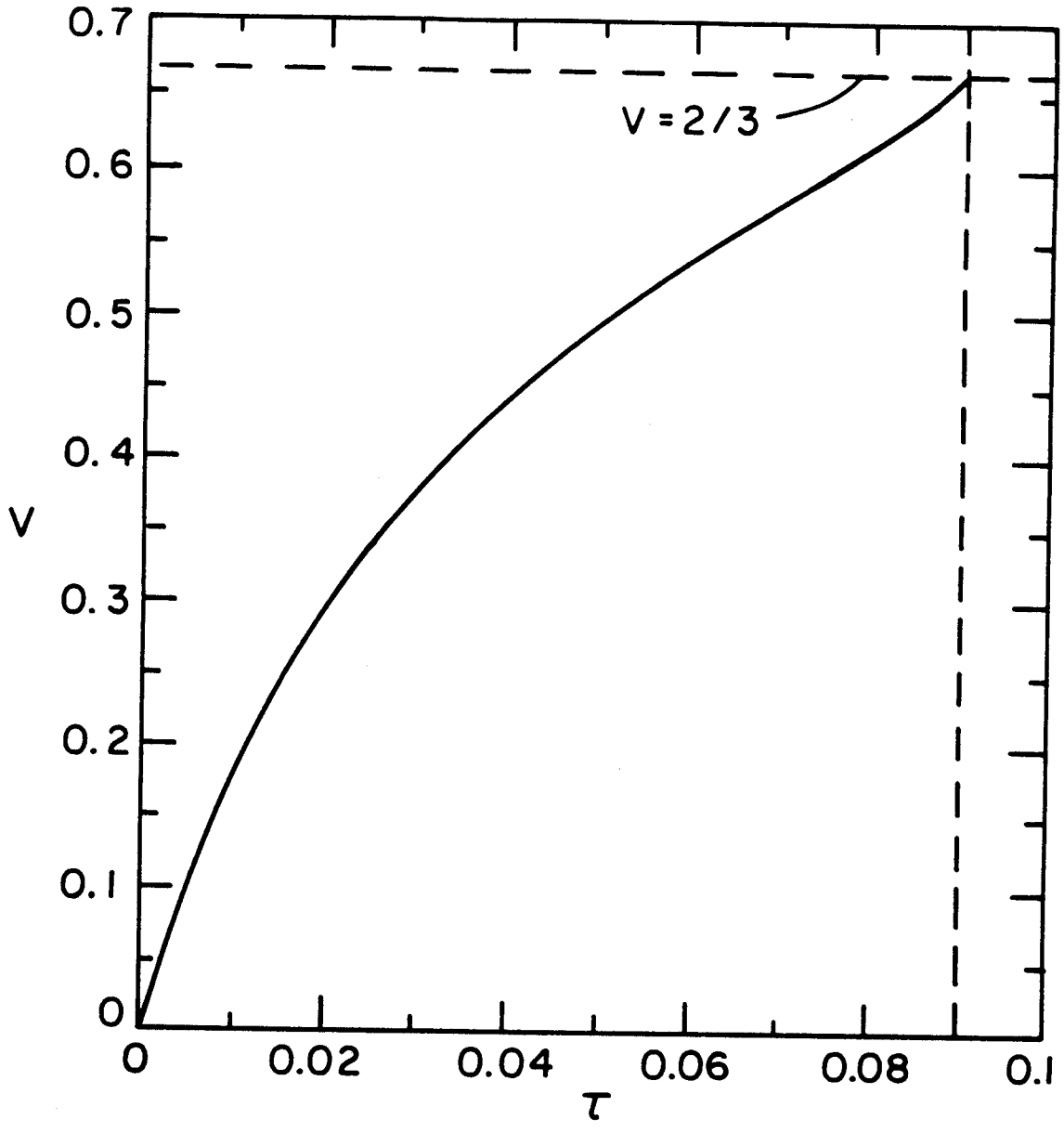

Fig. 9 $V(\tau)$ vs τ at the marginal stability point $\alpha\lambda^2 = 42/13$. The superconductor goes normal when $V = 2/3$.

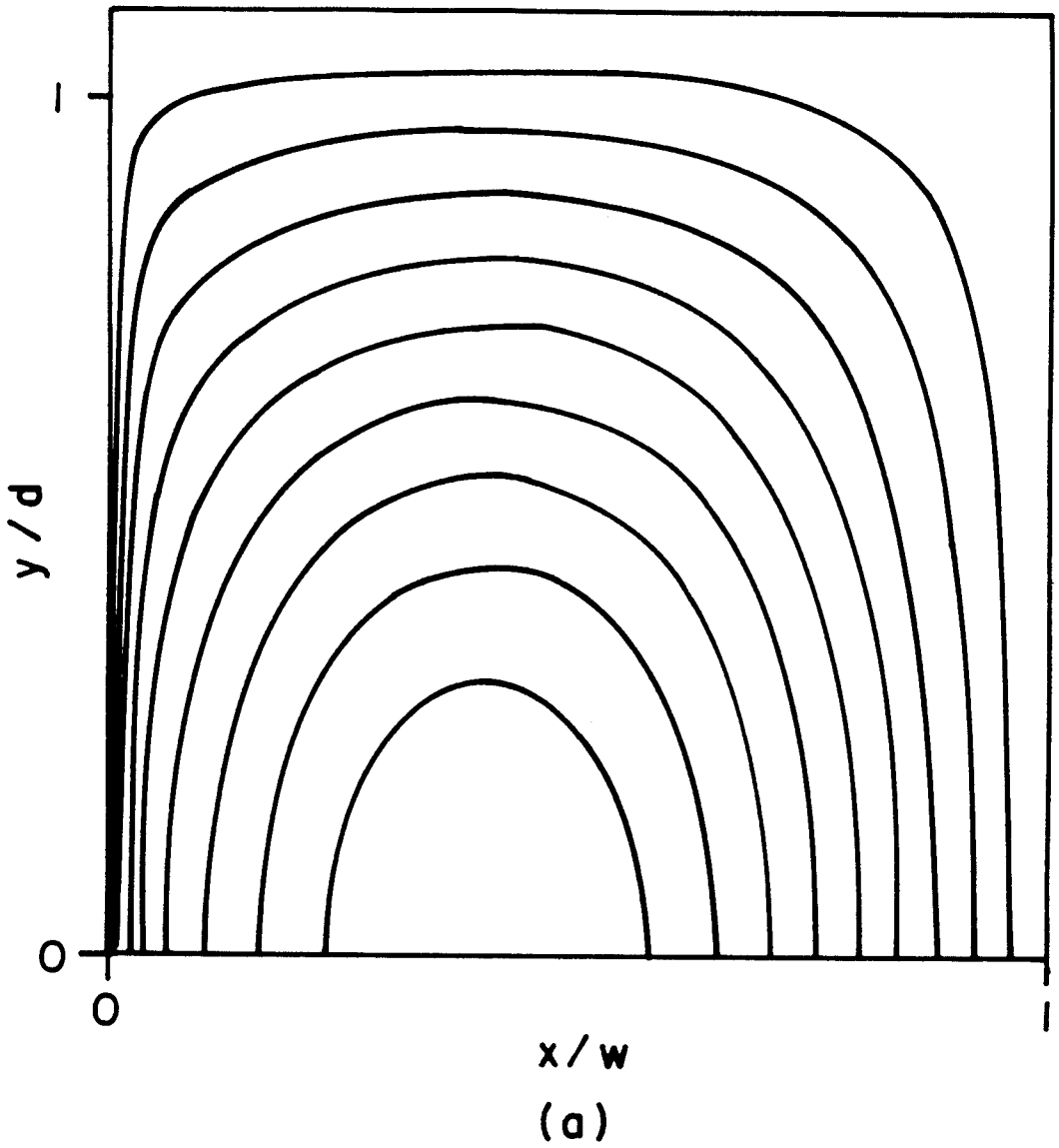

Fig. 10a Contour plots of $U_1(\rho, \zeta)$.

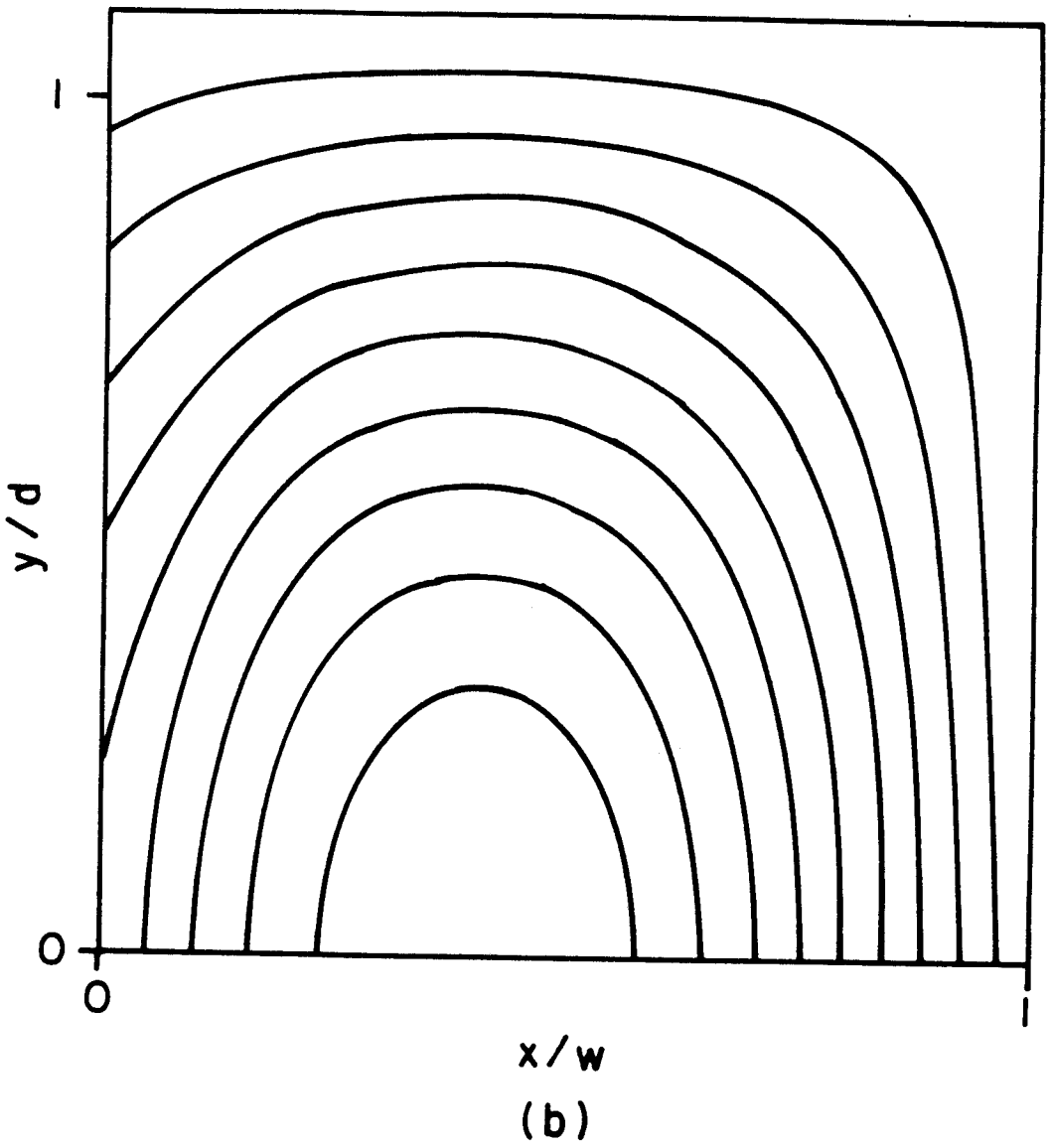

Fig. 10b Contour plots of $\psi_1(\rho, \zeta)$ for the case $\alpha = 10^3$, $\lambda = 0.5$, $\Gamma \to \infty$.

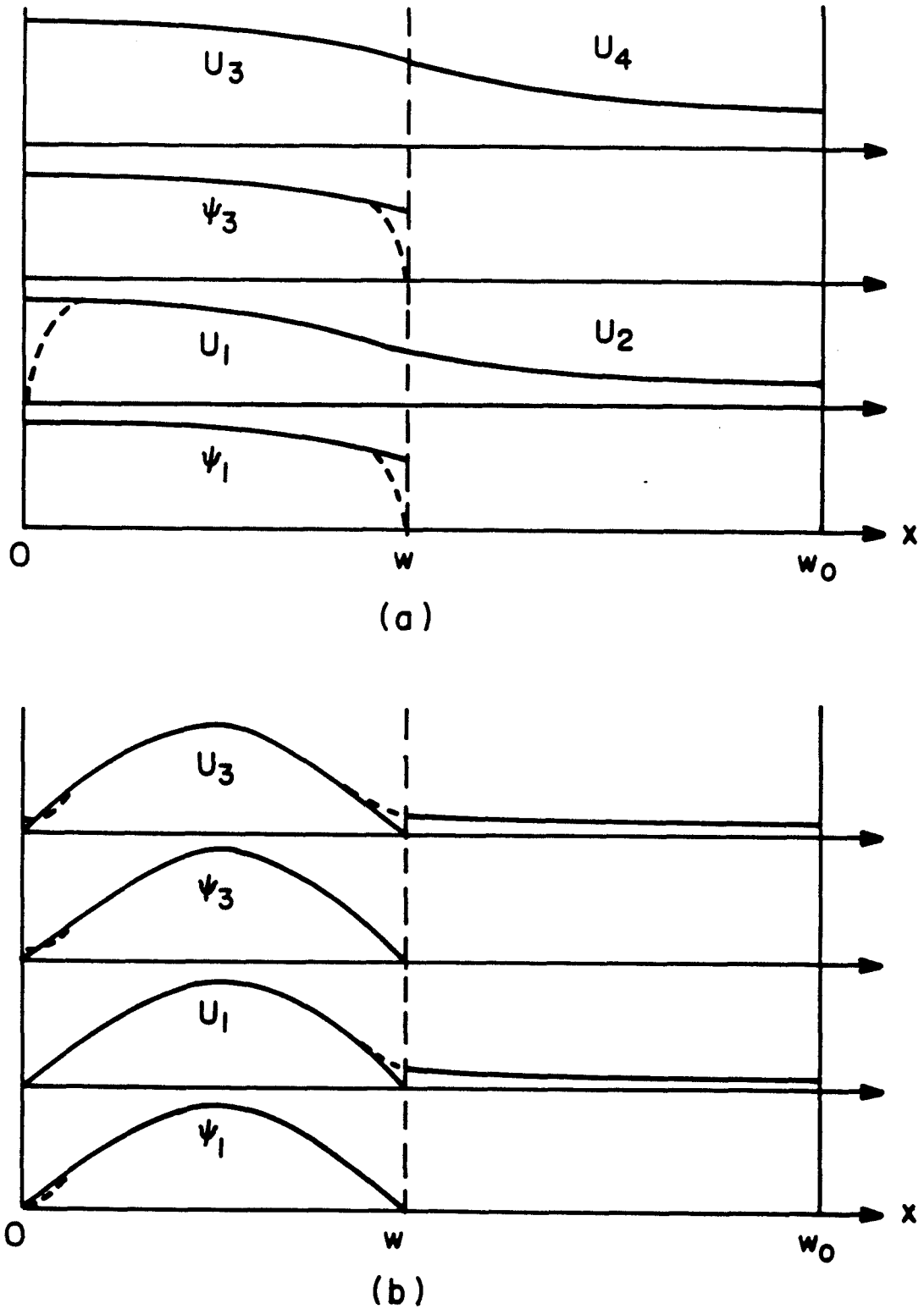

Fig. 11 Sketch of $U_j(\rho,1), \psi_j(\rho,1)$ vs ρ for (a) the U_3 boundary conditions at $\rho = 0,1$ dominant and (b) the U_1 and ψ_1 boundary conditions at $\rho = 0,1$ dominant.

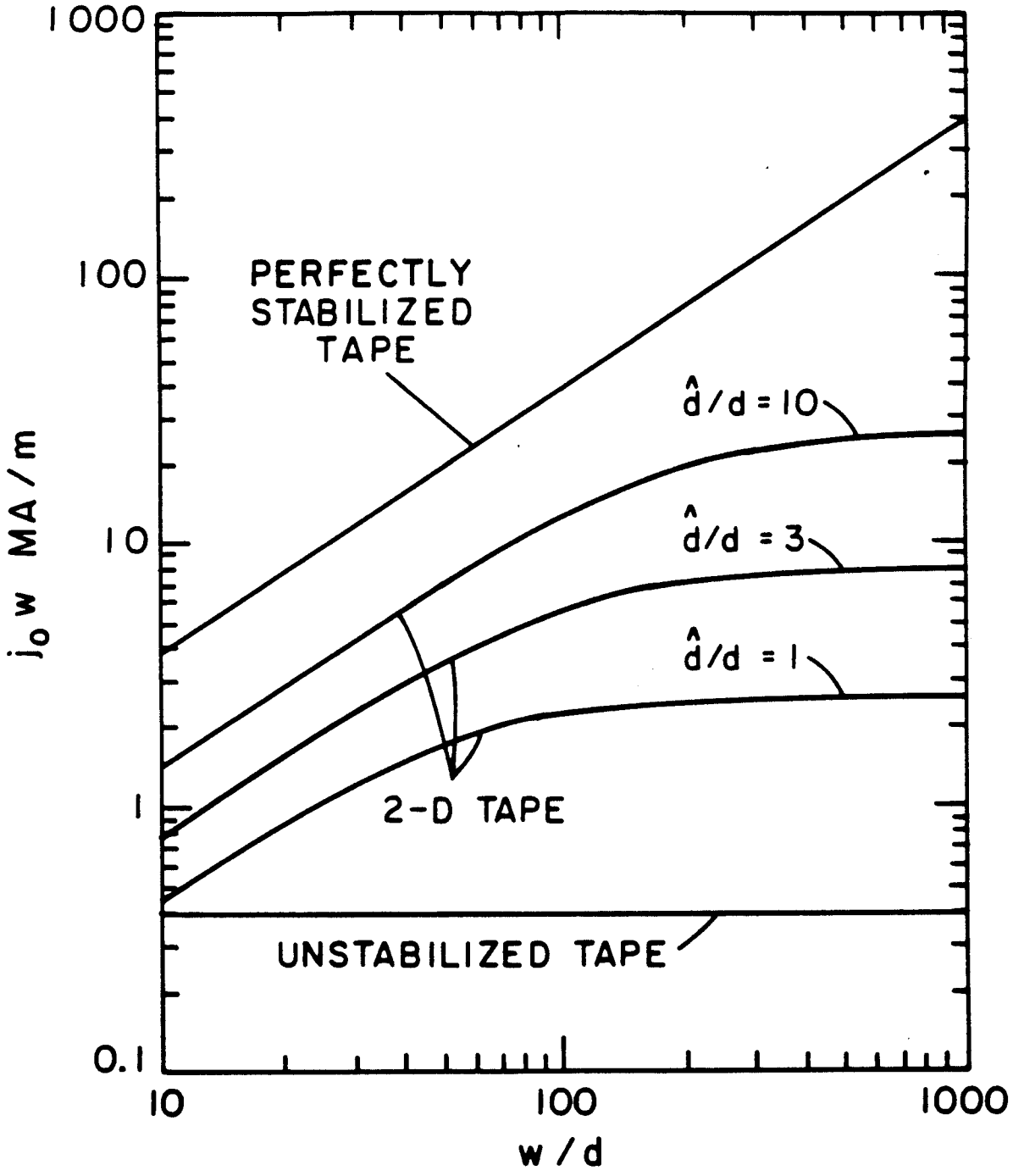

Fig. 12 Curves of critical $J_0 w$ vs w/d for various $\hat{d}/d$.